491 BAW

File Jel

3900

DA-36-039-SC-85122

Coordinated Science Laboratory

UNIVERSITY OF ILLINOIS - URBANA, ILLINOIS

TUNNEL DIODE DETECTOR

Prepared by

T. YASUI AND W. MAYEDA

REPORT R-138 MAY, 1962

COORDINATED SCIENCE LABORATORY
UNIVERSITY OF ILLINOIS
URBANA, ILLINOIS

Contract DA-36-039-SC-85122
D/A Sub-Task 3-99-01-002

The research reported in this document was made possible by support extended to the University of Illinois, Coordinated Science Laboratory, jointly by the Department of the Army (Signal Corps and Ordnance Corps), Department of the Navy (Office of Naval Research), and the Department of the Air Force (Office of Scientific Research, Air Research and Development Command) under Signal Corps Contract DA-36-039-SC-85122.

ABSTRACT

By use of a tunnel diode, it is possible to design a detector which is capable of amplifying a detected signal. Suppose input signal is an amplitude modulated signal whose modulating signal is $e_s \sin \omega_i t$ and the degree of modulation is very small. From the experimental results, the insertion gain

$$g_s = \left| \frac{e_o}{e_o'} \right|$$

is larger than 14 where e_o is the peak value of output signal corresponding to e_s with a tunnel diode being active and e_o' is the peak value of output signal corresponding to e_s with the tunnel diode being shorted.

TABLE OF CONTENTS

LIST OF ILLUSTRATIONS

1. INTRODUCTION

The use of only the negative resistance region of V-I characteristic of a tunnel diode, amplifiers[1-8] and oscillators[9-12] can be designed. By using only the positive regions, tunnel diodes can be used as bistable devices.[13-16] If both positive and negative resistance regions are used, a tunnel diode can be used as a detector which is capable of amplifying detected signal.[17-18]

This paper shows the principle of tunnel diode detectors and analytic and experimental results of such a detector with commercially available tunnel diodes.

2. PRINCIPLE OF TUNNEL DIODE DETECTOR

There are two typical circuits for tunnel diode amplifiers.[3] One is the series amplifier and the other is the parallel amplifier as shown in Fig. 1 a and b respectively.

Since the amplification by tunnel diodes is possible only because of the negative resistance of the diode, the biasing point must be set on the middle of the negative resistance region so that in each half cycle of input signal, the operating point A swings inside the negative resistance region as shown in Fig. 2a.

The idea of our detector circuit is to set the biasing point at the end of the negative characteristic, B or C, as shown in Figure 2b, so that this circuit acts as amplifier at a half cycle of input signal and acts as attenuator at the other half cycle.

In the paper the circuit (a) in Fig. 1 is used to perform detection by the proper setting of biasing voltage. However, it is also possible to use the circuit (b) in Fig. 1 to use as a detector. An equivalent circuit for such a detector is show in Fig. 3.

3. GAIN OF DETECTORS

Suppose the bias point of the diode in the circuit in Fig. 3 is set at the point B in Fig. 2. Then the gain of the circuit can approximately be calculated by considering the characteristic of the diode as the inverse of capital letter V as shown in Fig. 4a. Furthermore by proper transformation, the characteristic of the diode can be assumed to be the one shown in Fig. 4b and the circuit in Fig. 3 becomes the circuit in Fig. 5.

When the operating point is in the negative resistance region, the following equations from the circuit in Fig. 4b can be obtained:

$$\left.\begin{aligned} v_d^+ &= -iR_t - L_t \frac{di}{dt} + v_{in} \\ i^+ &= C_d \frac{dv_d}{dt} - \frac{v_d}{R_d} \end{aligned}\right\} \quad (1)$$

for $v_d \geq 0$ where

$$v_{in} = V_i \sin \omega t \quad (2)$$

and

$$R_t = R'_g + R_L \quad (3)$$

From these,

$$\frac{d^2 v_d^+}{dt^2} + \left(\frac{R_t}{L_t} - \frac{1}{R_d C_d} \right) \frac{dv_d^+}{dt} + \frac{R_d - R_t}{L_t C_d R_d} v_d^+ = \frac{V_i \sin \omega t}{L_t C_d} \quad (4)$$

The solution v_d of Eq. 4 is

$$v_d^+ = Ae^{\alpha_1 t} + Be^{\alpha_2 t} + \frac{(V_i/L_T C_d) \sin (\omega t - \beta)}{\sqrt{(b - \omega^2)^2 + \omega^2 a^2}} \quad \text{for } v_d \geq 0 \quad (5)$$

where A, B are arbitrary constants

$$\alpha_1, \alpha_2 = \frac{1}{2} (-a \pm \sqrt{a^2 - 4b}) \quad (6)$$

$$a = \frac{R_t}{L_t} - \frac{1}{R_d C_d} \quad (7)$$

$$b = \frac{R_d - R_t}{L_t C_d R_d} \tag{8}$$

and

$$\beta = \tan^{-1} \frac{\omega a}{b-\omega^2} \tag{9}$$

From the Eq.'s 9 and 12,

$$i^+ = (C_d\alpha_1 - \frac{1}{R_d})\ Ae^{\alpha_1 t} + (C_d\alpha_2 - \frac{1}{R_d})\ Be^{\alpha_2 t}$$

$$+ \frac{\frac{V_i}{L_t C_d}}{\sqrt{(b-\omega^2)^2 + \omega^2 a^2}} \left\{ \omega \cos(\omega t-\beta) - \frac{1}{R_d} \sin(\omega t-\beta) \right\} \tag{10}$$

and output voltage is obtained by $i^+ \times R_L$.

$$v^+_{out} = i^+ \times R_L \tag{11}$$

When the operating point is in the positive resistance region, the following equations can be obtained by replacing $-R_d$ by R_d in Eq.'s 2 and 11.

Therefore,

$$v_d = C \cdot e^{\alpha_1' t} + D \cdot e^{\alpha_2' t} + \frac{\frac{V_i}{L_t C_d} \sin(\omega t-\beta')}{\sqrt{(b'-\omega^2)^2 + \omega^2 a'^2}} \quad \text{for } v_d \leq 0 \tag{12}$$

where C and D are arbitrary constants

$$\alpha_1', \alpha_2' = \frac{1}{2} (-a' \pm \sqrt{a'^2 - 4b'}) \tag{13}$$

$$a' = \frac{R_t}{L_t} + \frac{1}{R_d C_d} \tag{14}$$

$$b' = \frac{R_d R_t}{L_t C_d R_d} \tag{15}$$

and

$$\beta' = \frac{a'\omega}{b'-\omega^2} \tag{16}$$

Similarly

$$i^- = (C_d \alpha_i' + \frac{1}{Rd})\, C \cdot e^{\alpha_1' t} + C_d \alpha_2' + \frac{1}{R_d})\, D\, e^{\alpha_2' t}$$

$$+ \frac{\frac{V_i}{L_t C_d}}{\sqrt{(b'-\omega^2)^2 + \omega^2 a'^2}} \left\{ \omega \cos(\omega t - \beta') + \frac{1}{R_d} \sin(\omega t - \beta') \right\} \tag{17}$$

and

$$v^-_{out} = i^- \times R_L \tag{18}$$

In order to make this circuit stable, it is necessary that the real part of roots α , α , α ', and α should be negative and in that case, the transient terms in Eq.'s 10 and 17 will vanish. Suppose A,B,C and D are not infinite. Then,

$$v^+_{out} \cong \frac{\frac{V_i R_L}{L_t C_d}\sqrt{\omega + (1/R_d^2)}}{\sqrt{(b-\omega^2)^2 + \omega^2 a^2}} \sin(\omega t - \beta - \gamma) \quad \text{as } t \rightarrow \infty \tag{19}$$

where

$$\gamma = \tan^{+} \omega \cdot R_d \sqrt{\omega^2 + \frac{1}{R_d^{\,2}}} \qquad (20)$$

Also

$$v^{-}_{out} \simeq \frac{(V_i R_L / L_t C_d) \sqrt{\omega^2 + \frac{1}{R_d^{\,2}}} \sin(\omega t - \beta' + \gamma)}{\sqrt{(b' - \omega^2)^2 + \omega^2 a'^2}} \quad \text{as } t \to \infty \qquad (21)$$

From the necessary condition that the circuit should be stable,

$$a = (R_t/L_t) - (1/R_d C_d) = \epsilon > 0 \qquad (22)$$

and from the condition that the circuit should be monostable,

$$b = (R_d - R_t/L_t C_d R_d) \geqq 0 \qquad (23)$$

For the circuit constants which satisfy Eq.'s 22 and 23, a' and b' become automatically

$$a' = (R_t/L_t) + (1/R_d C_d) > 0 \qquad (24)$$

$$b' = (R_d + R_t/L_t C_d R_d) > 0 \qquad (25)$$

Then, the real part of α_1' and α_2' can be negative and, therefore, this circuit is stable in the positive resistance region.

By expressing a' and b' by the terms of a and b, the equations

$$a' = a + \frac{2}{R_d C_d} \tag{26}$$

$$b' = -b + \frac{2}{L_t C_d} \tag{27}$$

can be obtained. By letter $b = \omega^2$, Eq.'s 7, 15, and 27 give

$$\therefore \quad \frac{1}{L_t C_o} = (\omega^2 + \frac{a}{R_d C_o} + \frac{1}{R_d^2 C_o^2}) \cong (\omega^2 + \frac{1}{R_d^2 C_o^2}) \tag{28}$$

for small a. Hence,

$$\left| \frac{v^-_{out}}{v^+_{out}} \right| \cong \frac{\omega \cdot \alpha R_d C_d}{2\sqrt{(\omega^2 + \frac{1}{R_d^2 C_d^2})}} \tag{29}$$

From Eq.'s 14 and 15 the following equations can be obtained

$$\omega^2 = (1/L_t C_d) - (a/C_d R_d) - (1/C_d R_d)^2) \tag{30}$$

Since

$$(a/C_d R_d) \ll 1/(C_d R_d)2 \tag{31}$$

$$\omega^2 \cong (1/L_t C_d) - (1/(C_d R_d)^2) \tag{32}$$

Substitution of this equation into Eq. 29 gives

$$\left|\frac{v^{-}_{out}}{v^{+}_{out}}\right| \cong (aC_o/2) \sqrt{R_d^{\,2} - (L_t/C_d)} \tag{33}$$

It is clear from Eq.'s 23 and 32 that a:

$$R_d^{\,2} - L_t/C_d \geq 0 \tag{34}$$

Eq. 33 shows that the ratio will decrease by decreasing C_d, R_d or by increasing L_t with fixed a, which means that better output waveform of a tunnel diode detector can be obtained either by decreasing C_o or R_d or by increasing L_t under the fixed a. However, it is known that a maximum L_t by the stability point of view. When the tunnel diode is shorted, the study state term of the current can be expressed as

$$i_s = \frac{V_i \sin(\omega t - \beta\delta)}{\sqrt{R_t^{\,2} + \omega^2 L_c^{\,2}}} \tag{35}$$

where

$$\delta = \tan^{-1} \frac{\omega L_c}{R_t} \tag{36}$$

Hence

$$v_{s\ out} = \frac{V_i R_L \sin(\omega t - \delta)}{\sqrt{R_t^{\,2} + \omega^2 L_c^{\,2}}} \tag{37}$$

Therefore, the ratio of $\left|V^{+}_{out}\right|$ and $\left|V_{s\ out}\right|$ which is an insertion voltage gain in detection circuit becomes

$$\left|\frac{v^+_{out}}{v_{s\ out}}\right| = \frac{\sqrt{R_t^{\,2} + \omega^2\ L_c^{\,2}}\ \cdot \sqrt{\omega^2 + (1/R_d)^2}}{L_t C_d \sqrt{(b-\omega 2)^2 + \omega^2\ a^2}} \qquad (38)$$

usually $L_c = 0$, hence

$$\left|\frac{v^+_{out}}{v_{s \cdot out}}\right| \cong \frac{R_t\ \cdot \sqrt{\omega + \frac{1}{R_d}2}}{L_t C_d \sqrt{(b-\omega^2)^2 + \omega^2 a^2}} \qquad (39)$$

If $R_L = R'_g$

$$\left|\frac{v^+_{out}}{v_{s\ out}}\right| \cong 2 \cdot \left|\frac{v^+_{out}}{v_{in}}\right| \qquad (40)$$

4. NUMERICAL ANALYSIS OF TUNNEL DIODE DETECTORS

The previous section shows the conditions by which the maximum detection ratio can be obtained from tunnel diode detectors by assuming the characteristic of the diode as an inverted capital letter v. Since a tunnel diode does not have such a characteristic the conditions given in previous section may not be proper conditions in order to design special purpose tunnel diode detectors which will be seen later. In order to design high gain tunnel diode detectors, it is necessary to investigate the relationship between the parameters in the circuit and output signals under the actual tunnel diode characteristics which can be done either by experimental set up or by numerical analysis.

In the experiment, it is difficult to adjust the values of circuit constants like c_d, L_c, R_t and so on as they are desired. However, when the circuits are analyzed by the computer, it is possible to control them. Furthermore, it is also possible to analyze the circuit with the ideal elements.

From the circuit in Fig. 3, the following equations can be obtained:

$$L_t \frac{di}{dt} + R_t i + v_d = v_i \sin \omega t + E \tag{41}$$

$$C_d \frac{dv_d}{dt} = i - i_d(v_d) \tag{42}$$

Combining above equations, Eq. 43 can be obtained.

$$\frac{d^2 v_d}{dt} + \frac{R_t}{L_t} \frac{dv_d}{dt} + \frac{v_d}{L_t C_d} + \frac{1}{C_d} \frac{di_d(v_d)}{dt}$$

$$+ \frac{R_t}{L_t C_d} i_d(v_d) - v_i \sin \omega t + E \tag{43}$$

By the use of a digital computer, Eq. 43 can be solved with parameters R_t, L_t, C_d, V_i, ω and E and characteristic $i_d(v_d)$ of a tunnel diode as shown in Fig. 6.

$-R_d$ at P is approximately equal to 100 Ω. The junction capacitor C_o of such a tunnel diode is approximately $C_d = 6 \times 10^{-12}$ f (which is estimated by considering present A_s tunnel diode). The frequence ω of the input signal $V_i \sin \omega t + E$ is set to $2\pi \times 10^8$ cps for convenience. From Eq.'s 7 and 8, the following equation can be obtained:

$$R_t = \frac{(R_d C_d\, a + 1) R_d}{\omega^2 (C_d R_d)^2 + a\, R_d C_d + 1} \qquad (42)$$

and

$$L_t = \frac{R_t R_d C_d}{(a R_d C_d + 1)} \qquad (43)$$

For convenience, R_{t_o} is defined as

$$R_{t_o} = \frac{R_d}{\omega^2 C_d^2 R_d^2 + 1}. \qquad (44)$$

Also L_{t_o} is defined as

$$L_{t_o} = R_t R_t C_d \qquad (45)$$

Notice that $R_t \cong R_{t_o}$ and $L_t = L_{t_o}$ if $a \ll \frac{1}{R_d C_o}$. Also $R_t > R_{t_o}$ and $L_t > L_{t_o}$ for $a > o$ with fixed ω. Then the values $R_d = 100\,\Omega$, $C_d = 6 \times 10^{12}$f, and $\omega = 2 \times 10^8$ cps, R_{t_o} and L_{t_o} are approximately equal to 87.6 ohms and 5.25×10^{-8} h respectively.

The following are the results obtained by the numerical calculation using a digital computer:

(i) R_t v.s. v_{out}

By varying R_t, the curve in Fig. 7 is obtained. L_t is also varied in order to make an invarient.

Notice that R_{t_o} gives maximum v^+_{out} by Eq.'s 19 and 20. From the curve in Fig. 7 it is clear that $R_t > R_{t_o}$ gives larger v^+_{out} which means that the conditions obtained by linealized characteristics of tunnel diodes are not applicable for the designing of a tunnel diode and detector.

The reasons are as follows: (1) because the negative resistance region is finite, the magnitude of the output signal under the situation that the operating point would be inside of the negative region is bounded which makes finite magnitude at output signal; (2) since the magnitude of the negative resistance near the peak current is larger than that near the middle point of the negative resistance region, with the small signal input and with the biasing point at the peak current region, larger R_T should give the larger output voltage than R_t which is almost equal to R_d.

(ii) Biasing Point vs. Vout.

When the biasing points of the tunnel diode in Fig. 2 are varied from C to A to B as shown in Fig. 8, the wave form of output voltage Vout will be changed as in Fig. 9.

(1) When the biasing point is at B(V_B = .06V in Fig. 8) the positive side of the output voltage v^+_{out} is a little larger than that when V_B = 05V. However, the negative side of output voltage v^-_{out} is also larger than that when V_B = .05 V.

Hence, as far as detection is concerned biasing at the peak current region would be better than biasing at the point which is away from the peak current region such as C or B in Fig. 8.

(iii) Input voltage vs. Output voltage

The curves in Fig. 10 show that v_{in} vs. v_{out} with different values of parameters. Every curve in the figure shows the sudden increase of gain which can be seen in the experimental results shown in the next section. After sudden increase the operating point will reach to the valley region of the characteristic curve in Fig. 8 which makes the detector circuit into saturating states(the output voltage will not increase by increasing the input voltage). Notice that even though $a < 0$, the circuit will not be unstable with small input signal which contradicts the results in the previous section.

(iv) L_t vs. V_{out}

With $R_t = 114\,\Omega$ and $C_o = 6$ PF, the curve in Fig. 11 is obtained. Even though $R_t > R_d$, the circuit will act as a detector with small input signals. It is important to notice that the increase of L_t will increase the output voltage v_{out}. However with $V_i = 10$ mv, the end of the right hand side of the curve is approaching the saturation point of the circuit. Also, L_t must be small enough to avoid self-oscillation.

5. EXPERIMENTAL RESULTS

The calculation of Eq. 4 by a digital computer for a large number of combinations of different values of parameters in the tunnel diode detector needs a large amount of time. Also, in order to verify that the results from the calculation by a computer are applicable to design a tunnel diode detector, the following experiment is carried out. The circuit scheme is shown in Figure 12.

(i) Miniature variable resistors were used as series resistors and by adjusting the value of these resistors, we investigated the relations between v_{out} and the values of the resistors R'_g and R_L.

In order to avoid any influence on the results by stray capacitances and conductances in the circuit to be measured, the carrier frequency of the amplitude modulated input signal is limited to 3 mc. The tunnel diode which is used in the circuit is GE 1N2939 which has about 1 ma peak current. The V-I characteristic of the diode which is traced by the curve traces shown in Fig. 13 is shown in Fig. 14.

According to the manual of the tunnel diode, the value of C_d and L_d of IN2939 are 5.0 to 1.5 μf and 6 nh respectively

The D. C. bias voltage of the tunnel diode is measured by the oscilloscope with differential amplifier.

(ii) For the bias voltage the output voltage of the power transistor which gives the smooth varying D.C. voltage by controlling the base current is used.

In order to obtain the output wave form as a function of the magnitude of the input signal, it is convenient to make V_i of input signal $V_i \sin 2\pi ft$ not as a constant but as a linearly increasing time varying signal. Hence the sawtooth wave with period of about 1 m sec is used which is easily obtained from the sawtooth wave output of the oscilloscope.

Table I shows the output waveform v_{out} corresponding to amplitude modulated wave with modulating signal being a sawtooth input waveform and carrier frequency of .5 mc for different values of R_t and biasing voltage V_B.

The symbol $v_{s\ out}$ is the output voltage when the tunnel diode is shorted. $v_{s\ out}$ of the circuit under experiment is as shown in Fig. 15.

If there is only one waveform in a picture in Table I, then the waveform indicates v_{out} and $v_{s\ out}$ are equal to that in Fig. 15. If there are two waveforms in a picture, one whose slope is an isosceles triangle is $v_{s\ out}$ and the other is v_{out}.

The unit of the vertical axis in every picture in the table and Fig. 15 is 5 mc except two pictures corresponding to R_t = 160 ohms and the biasing voltages of 80 mv and 165 mv (each of which has unit of the vertical axis 10 mv). The maximum peak to peak voltage of $v_{s\ out}$ in Fig. 15 in most of the pictures in Table I is, therefore, 15 mv except in the three pictures corresponding to R_t = 136 ohms and the biasing voltages of 100 mv, 120 mv and 140 mv (each of which has peak to peak $v_{s\ out}$ voltage of 5 mv).

From V-I characteristic of a tunnel diode in Fig. 14, the voltage v_d at the peak amount is about 70 mv. The biasing point at about 80 mv are where the point on the curve is a little away from the peak current toward to the valley current. The biasing voltages from 120 mv to 140 mv are where the point on the curve in Fig. 14 is about the middle on the negative resistance region at which the magnitude of the negative resistance is the minimum. The biasing voltage of 165 mv is the point at which the magnitude of the negative resistance begins to increase rapidly. Hence, at the biasing voltage between 100 mv and 140 mv in Table I, the circuit in Fig. 12 acts as a detector. The minimum negative resistance $-R_d$ of the tunnel diode in the circuit in Fig. 12 is between -135 ohms and -138 ohms. Hence there is the case which $R_t = 160 \gg R_d$. It is impossible to obtain pictures for which the biasing point is between 100 mv and 140 mv. The reason is simply that the circuit is unstable at these biasing voltages. Notice that the output signal increases suddenly in the pictures for the biasing voltages of 70 mv and 80 mv (R_t = 160 ohms).

For convenience, the symbol g_{s_i} is defined as

$$g_{s_i} = \frac{P_i}{q} \quad (i = 1,2) \tag{46}$$

where P_1 is the slope of the upper envelope and P_2 is the slope of the lower envelope at time t of the output waveform v_{out} in a picture in Table I in which the horizontal axis indicates time t, q is the slope of one side of envelope of $v_{s\ out}$ corresponding to the picture. Then it is clear from Table I that the max (g_{s_1}, g_{s_2}) is larger if R_t is larger when the biasing voltage V_B is one of 70 mv, 80 mv, and 165 mv.

Notice that g_{s_i} is a function of $v_{s_{out}}$.

Suppose $v_{s\ out}$ is as shown in Fig. 16a which indicates that the input signal to a tunnel diode is an amplitude modulated signal with very small degree of modulation. Also suppose v_{out} is as shown in Fig. 16 b. Then g_{s_i} is almost equal to e_o/e_s with very small e_s. Also the following equation will hold;

$$v_{out} = k + g_{s_i} v_{s_{out}} \tag{47}$$

where k and g_s are functions at $v_{s\ out}$. Hence k and g_{s_i} give the relationship between $v_{s\ out}$ and v_{out} which indicates the quality of detection, that is, for a small input signal e_s, larger g_{s_i} gives larger amplification (which means larger e_o). Notice that for small e_s, k is not important at all. However, for a larger e_s, constant g_{s_i} and k will be the best for a linear amplification of e_s.

Fig. 17a shows that g_{s_i} varies rather rapidly. Also it indicates that for higher frequency, maximum g_{s_1} does not change much for changing $v_{s\ out}$ near maximum g_{s_1} when the carrier frequency becomes higher.

From Eq. 19 it can be seen that there exists a critical frequency ω_c of carrier frequency where $\omega_c^2 = b$ in Eq. 19, such that with increasing carrier frequency ω above ω_c, the output v^+_{out} decreases. But increasing carrier frequency ω which is still below ω_c increases the output V^+_{out}. However, the results in Fig. 17a show that the increasing carrier frequency ω decreases v^+_{out} and g_{s_1}. Even ω is much less than ω_c.

Fig. 17a also shows the g_{s_2} of v_{out} corresponding to the negative half-cycle at the input signal by which the detection by the tested circuit is excellent. Fig. 17b shows the k of v_{out} corresponding to the positive and the negative half-cycle of the input signal respectively.

With carrier frequency ω = .5 mc, total series resistance R_t = 136 ohms, small signal gain g_s vs. input signal is shown in Fig. 18. From this it is learned that there are two regions on V-1 characteristics of a tunnel diode such that by setting biasing point in one of these two regions, the circuit becomes a detection with reasonably high gain obtainable. These two are regions near points B and C in Fig. 2b. Notice that at the region near point C in Fig. 2b, the output waveform v_{out} has $g_s > 2$ for half-cycle at which maximum (g_{s_1}, g_{s_2}) for the other half-cycle is obtained. On the other hand, at region near point B in Fig. 2b, $g_s < 1$ for a half-cycle at which maximum (g_{s_1},g_{s_2}) for the other half-cycle is obtained.

Fig. 19 shows how changing total series resistance R_t influences g_s vs. $v_{s\ out}$. Notice that when $R_t > r_{d_1}$ max (g_{s_1}) is large which is predictable from the pictures in Table 2 in which there is a sudden increase of v_{out}. For a comparison, the output waveforms of a carrier frequency by experiment and by the computation (by a digital computer) are shown in Fig. 20 a and b.

6. CONCLUSIONS

It is not difficult to design a tunnel diode detector with small signal gain g_s at about 15. Hence if the input signal is an amplitude modulated wave with small percentage of modulation, a tunnel diode detector is a very practical circuit which has advantages over an ordinal diode detector. There are many problems related to the detector which are left for future work. These problems are indicated in each section of this paper.

(a) Series amplifier (b) Parallel amplifier

Fig. 1

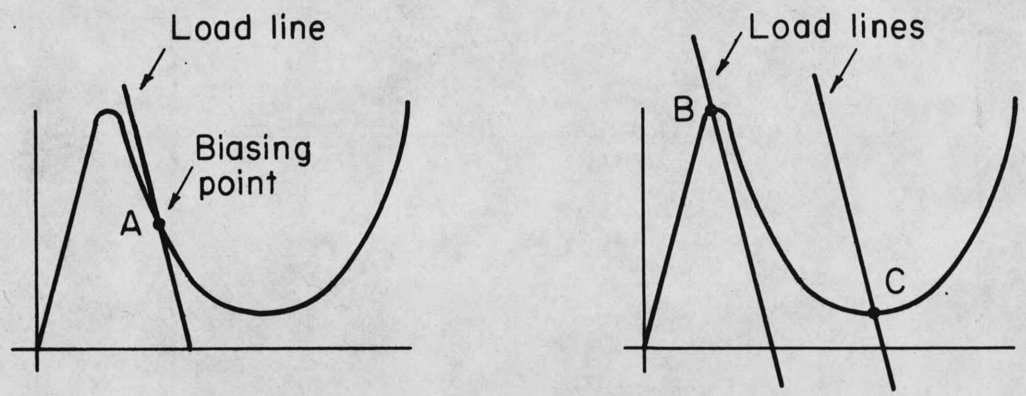

(a) Biasing point for usual amplifier

(b) The biasing points B or C for detector

Fig. 2

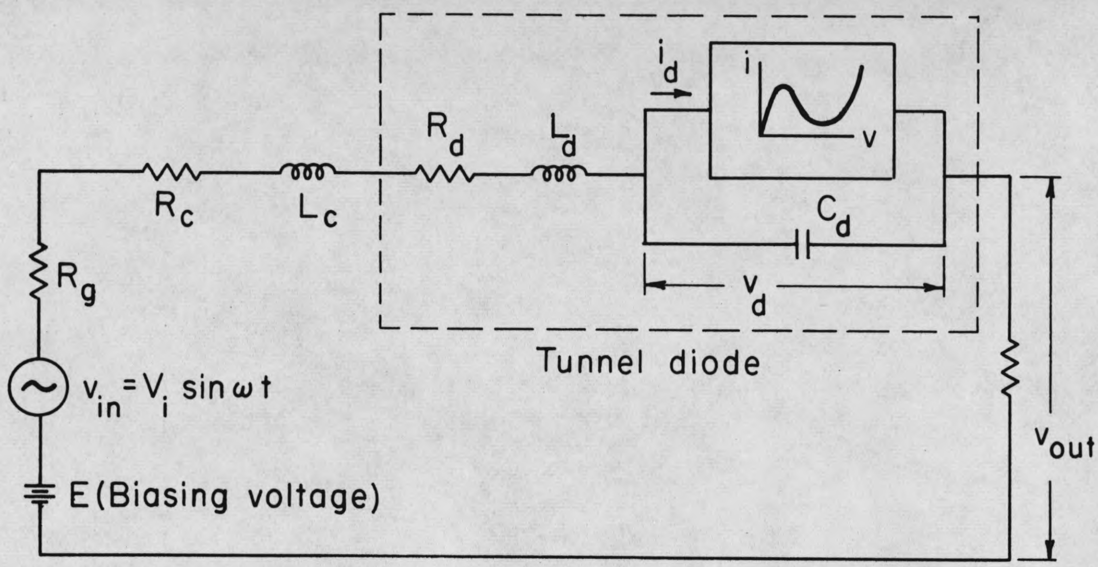

Fig. 3. Equivalent circuit for a tunnel diode detector

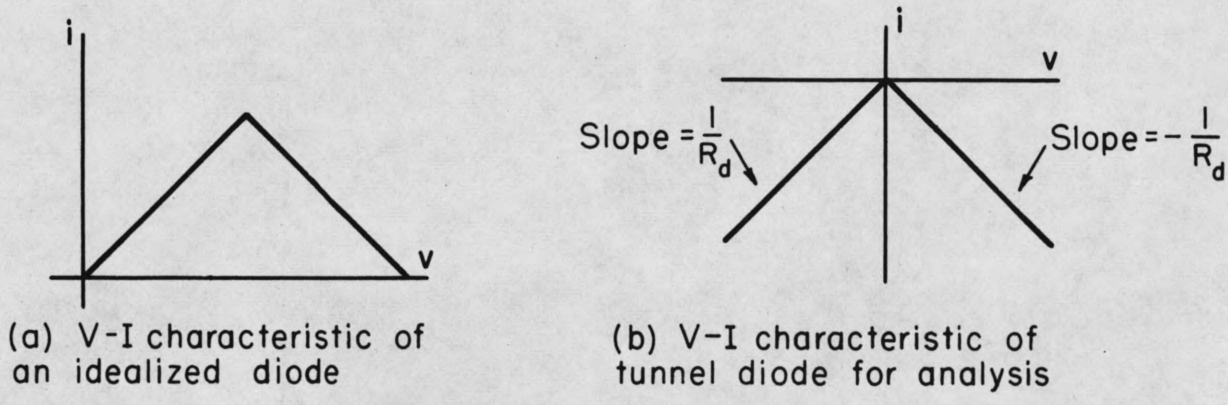

Fig. 4. Simplified V-I characteristic of a tunnel diode

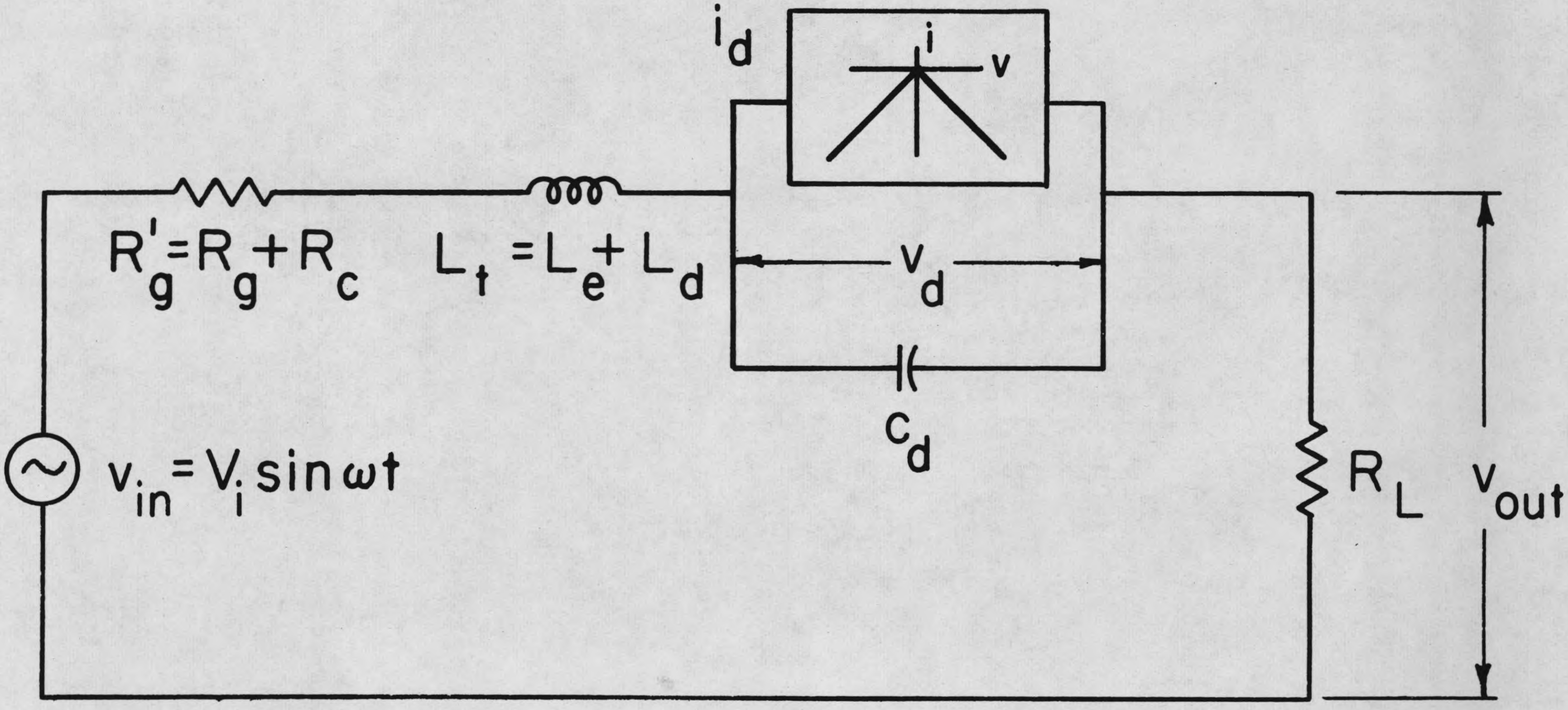

Fig. 5. Equivalent circuit for tunnel diode detector with specified B-I characteristic.

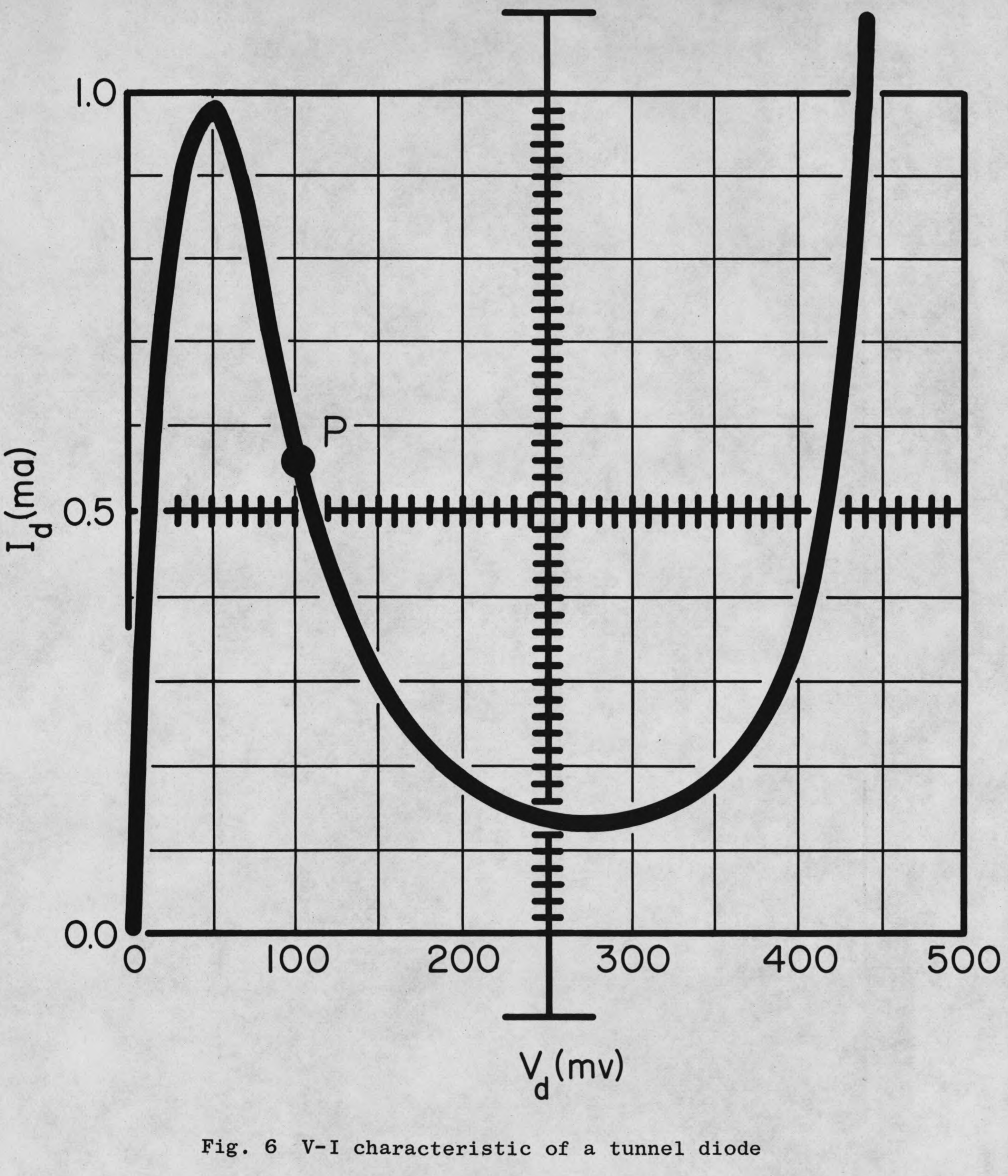

Fig. 6 V-I characteristic of a tunnel diode

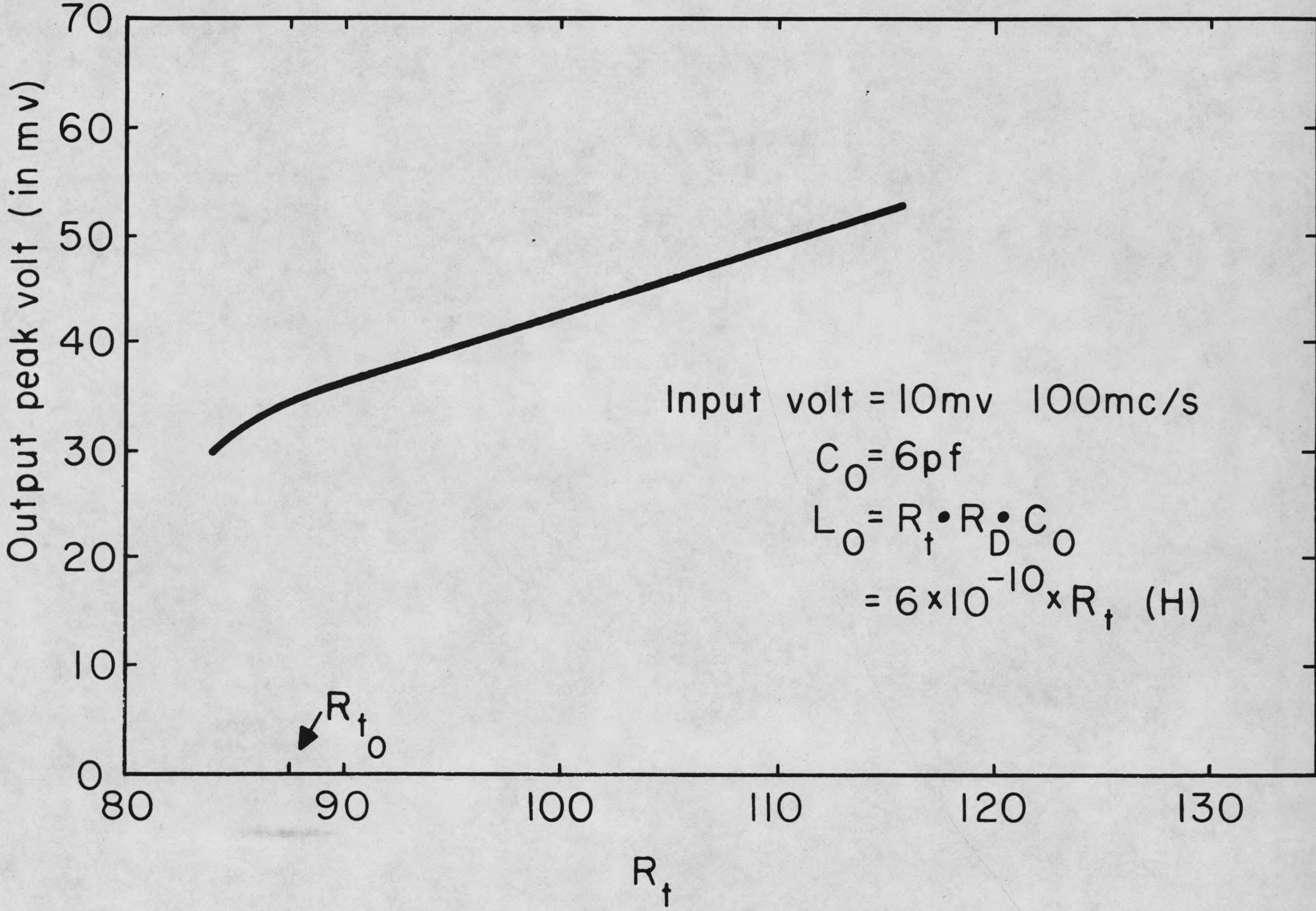

Fig. 7. Peak v_{out} v.s. R_t

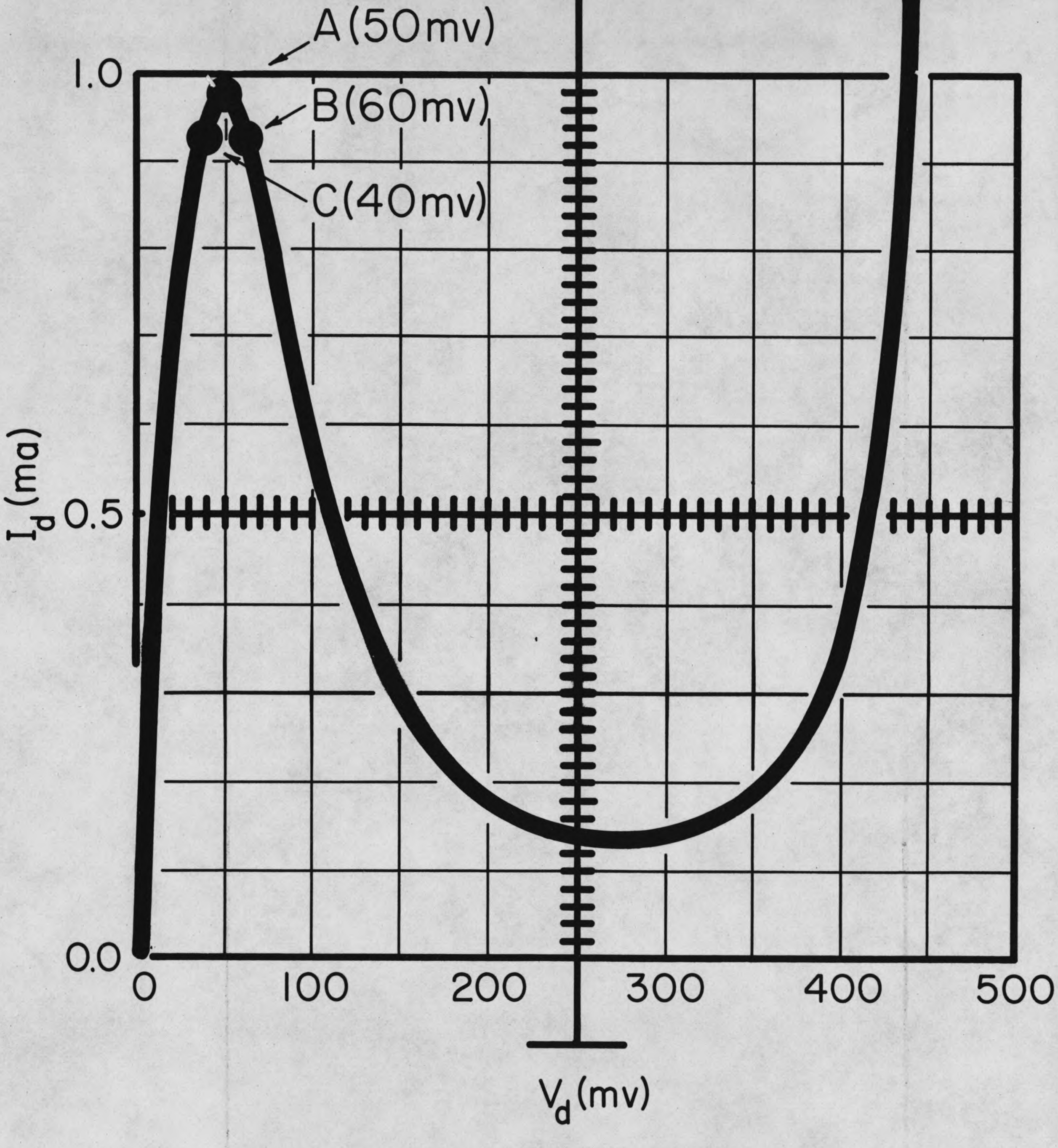

Fig. 8. Biasing Points A, B, and C.

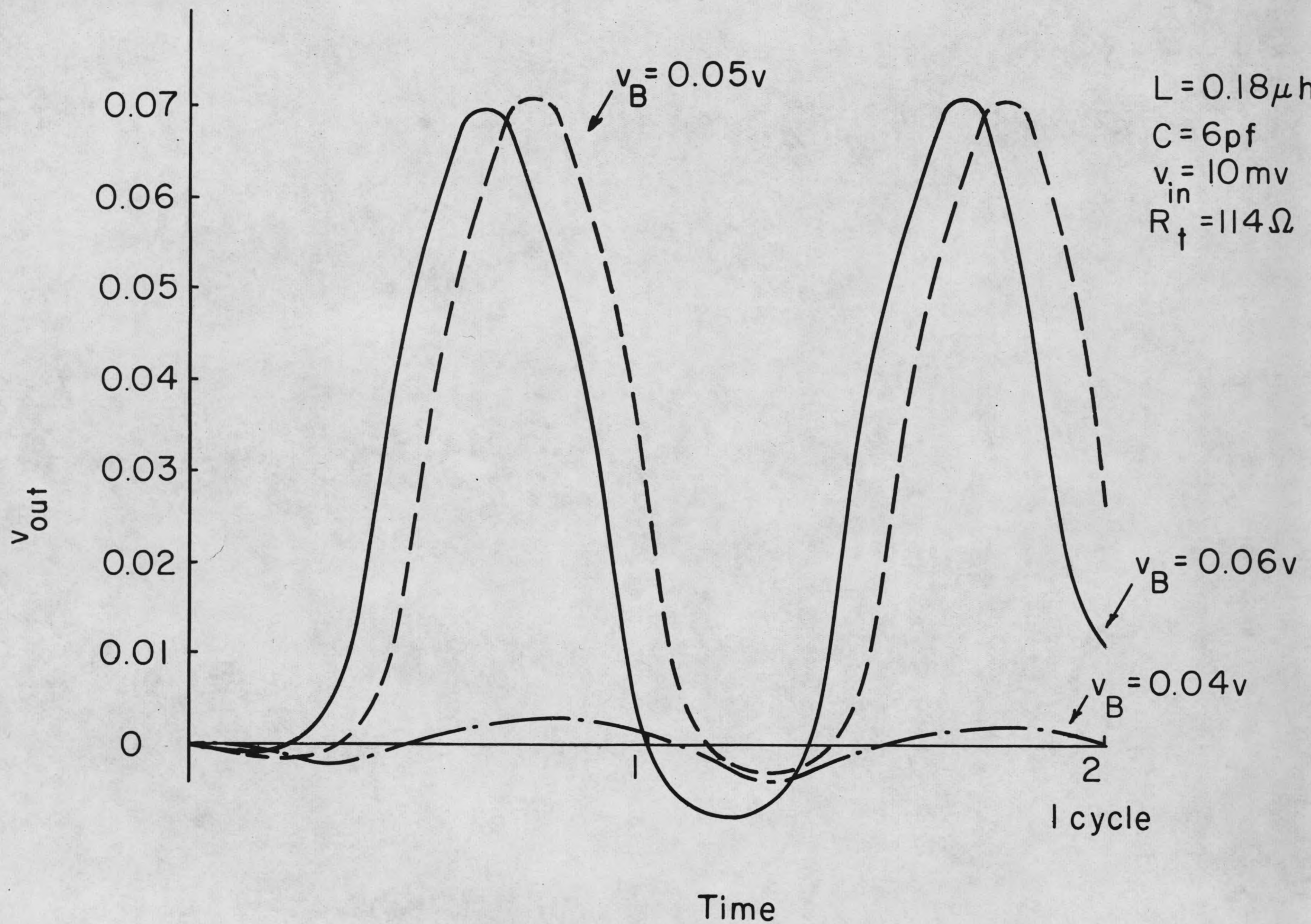

Fig. 9. Variation of v_{out} by different biasing points

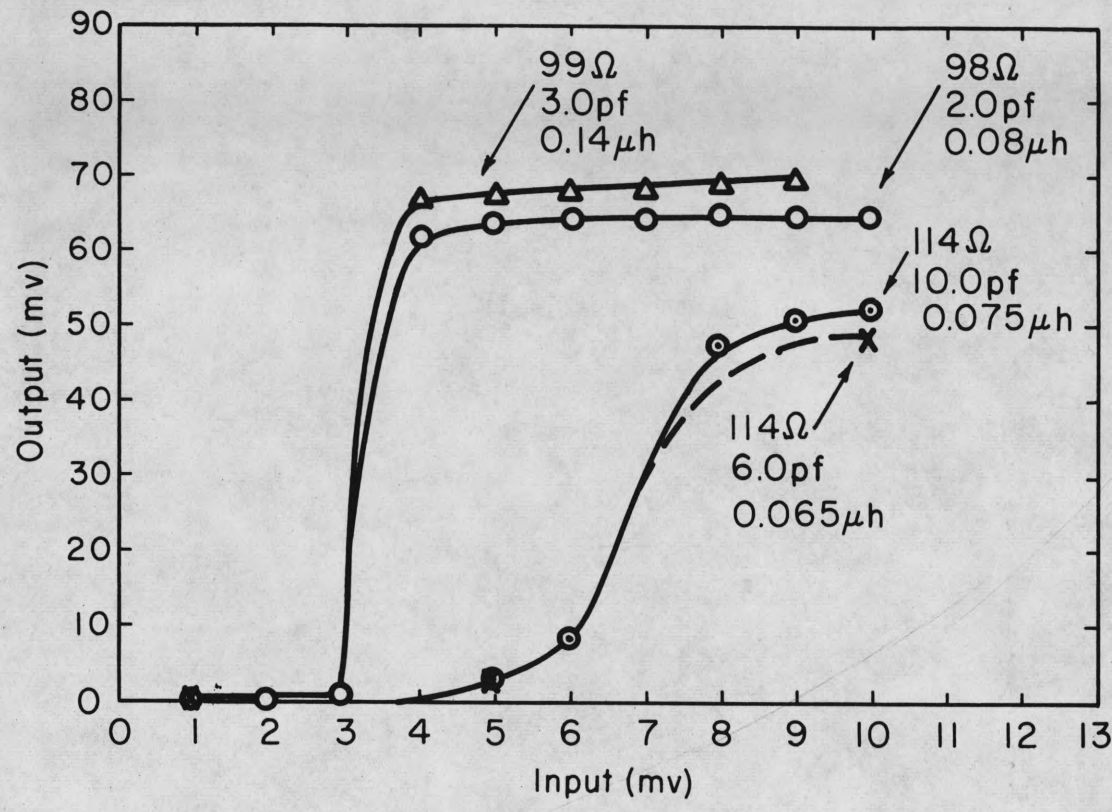

Fig. 10. v_{in} v.s. v_{out}

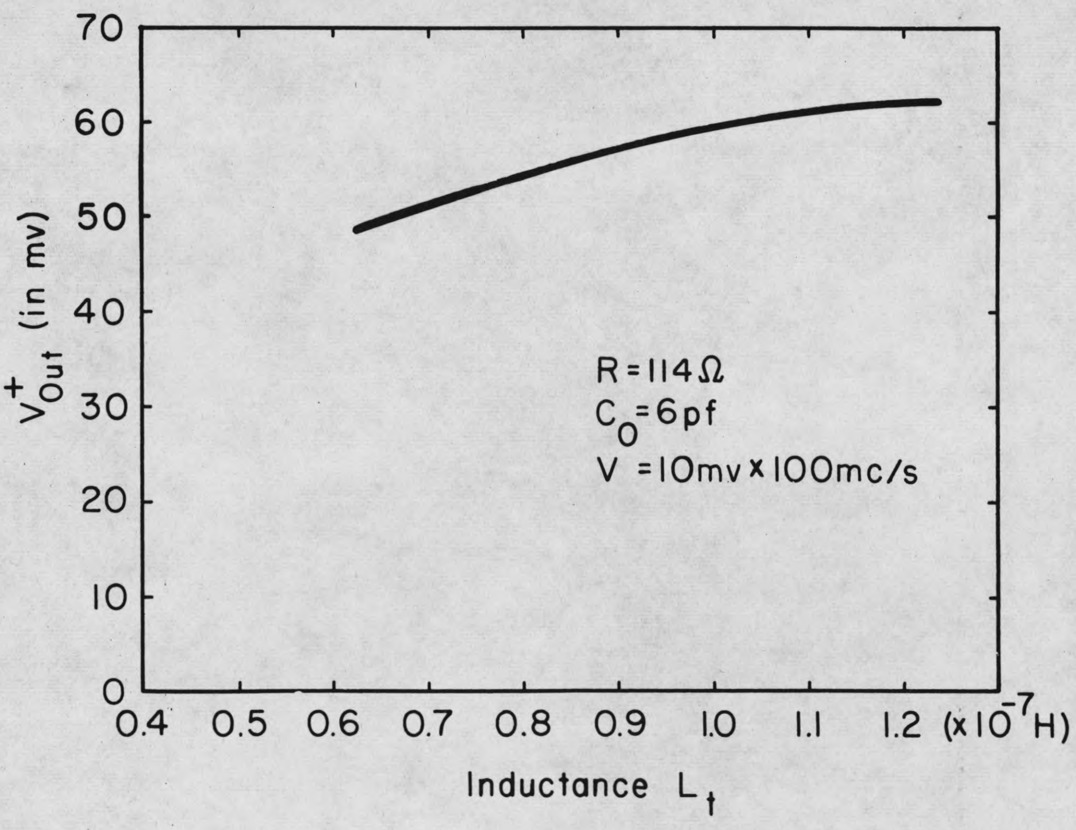

Fig. 11. v_{out} v.s. L_t

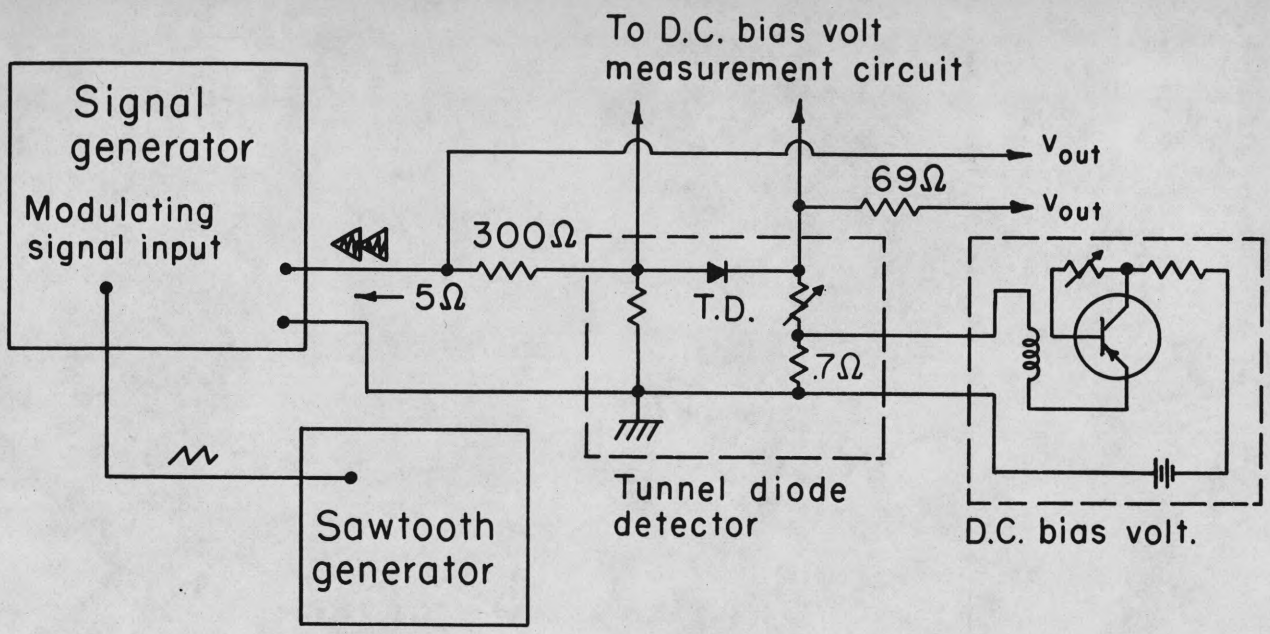

Fig. 12. Circuit scheme for testing a tunnel diode detector.

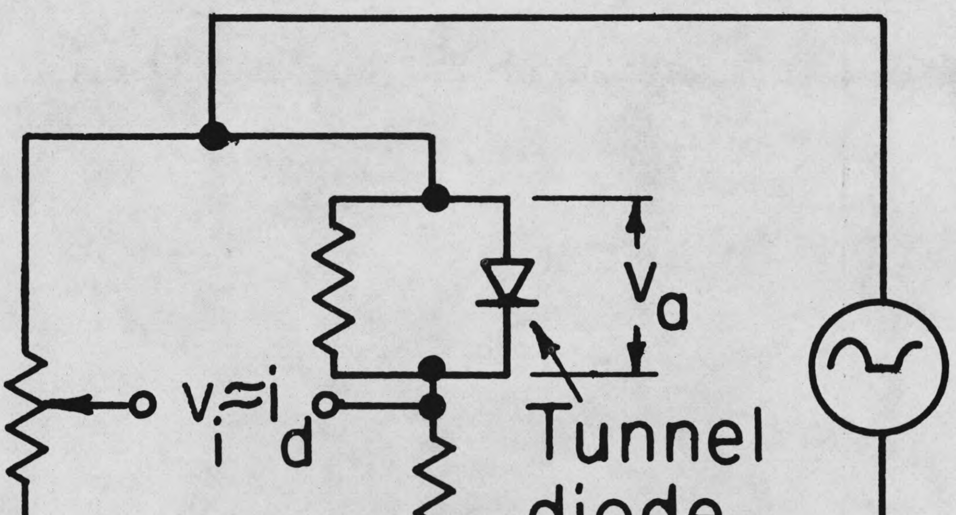

Fig. 13. Tunnel diode curve traces.

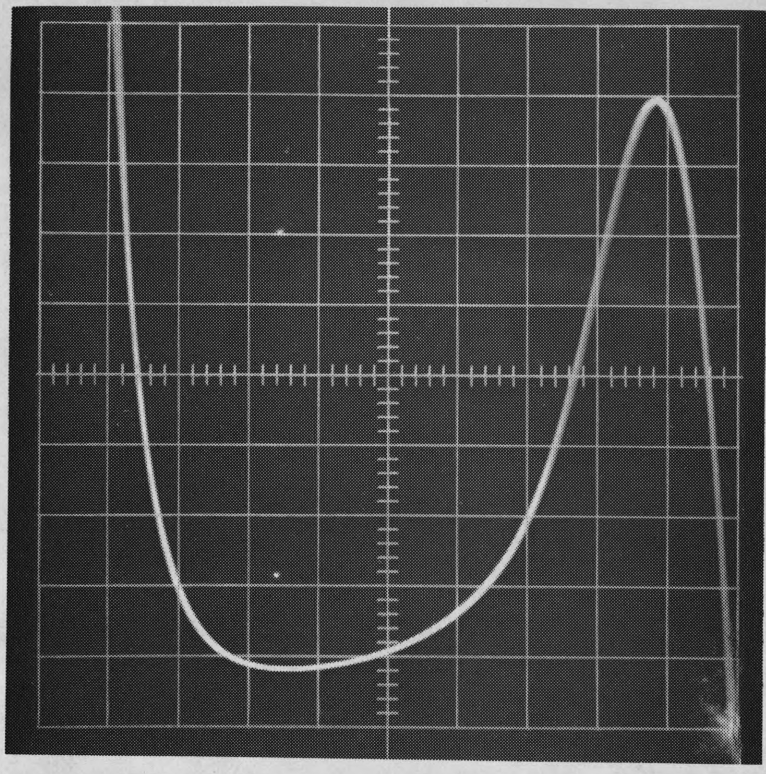

Fig. 14. V-I characteristic of 1N2939

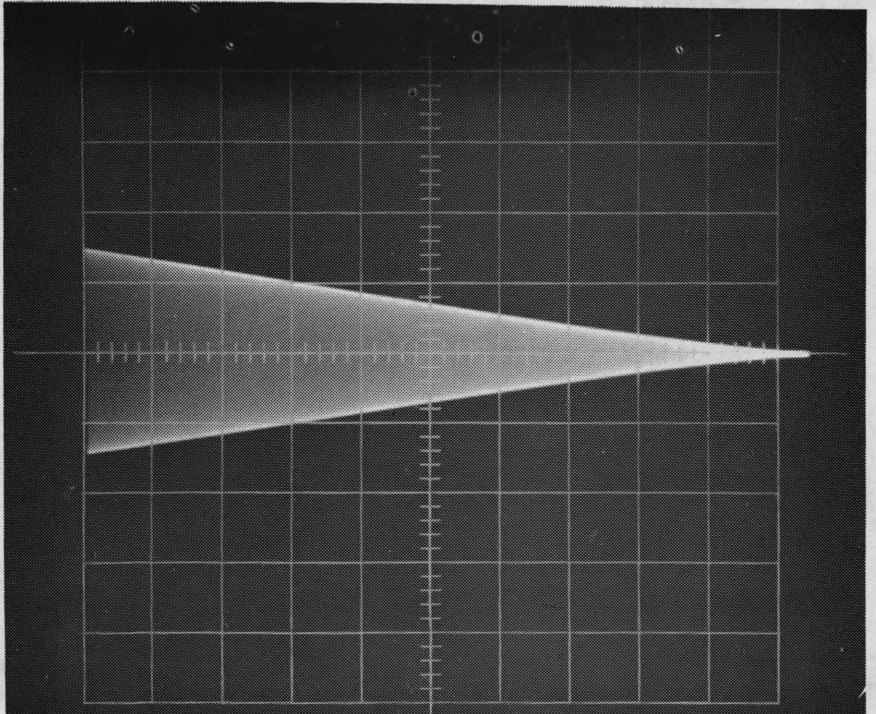

Fig. 15. Waveform of $v_{in}(t)$

Table 1

($R_T = R'_g + R_L$ and $R'_g \cong R_L$, V_B : Bias Voltage)

V_B (mv) \ R_T (ohm)	160	140	136	130	120
70	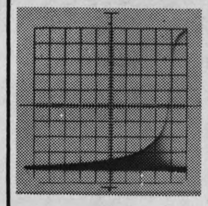	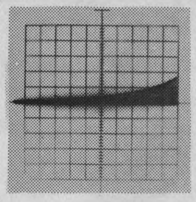	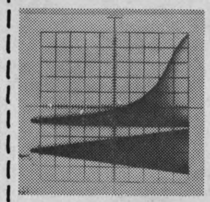	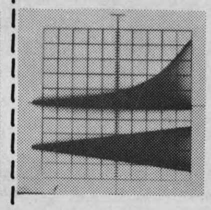	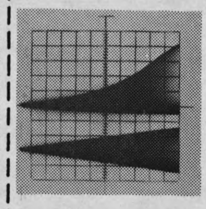
80	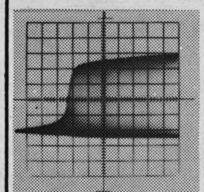 Vert. 10mv/Unit	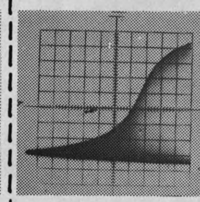	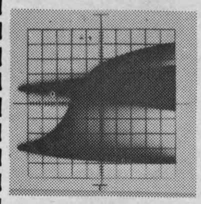	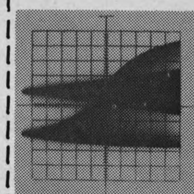	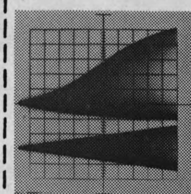
100		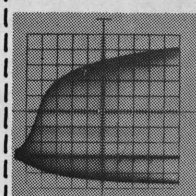	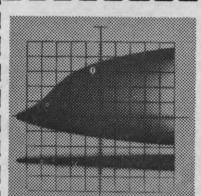 Max. $V_{S_{out}}$: 5mv p-p	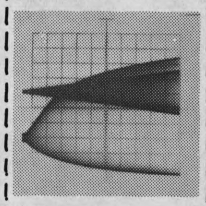	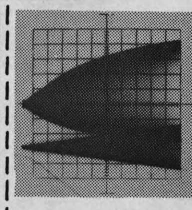
120		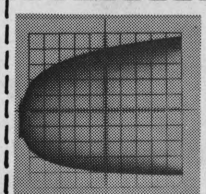	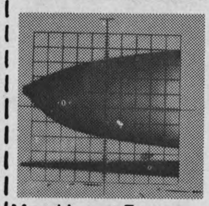 Max. $V_{S_{out}}$: 5mv p-p	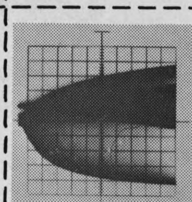	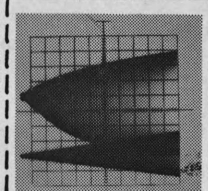
140		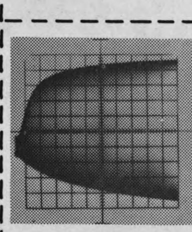	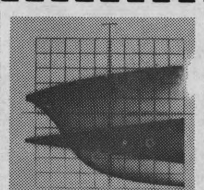 Max. $V_{S_{out}}$: 5mv p-p	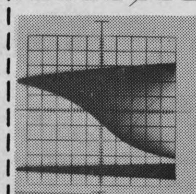	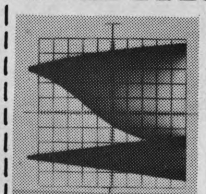
165	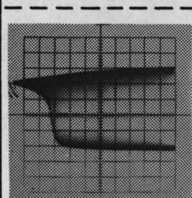 Vert. 10 mv/Unit	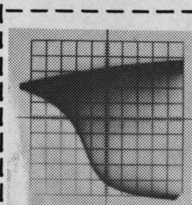	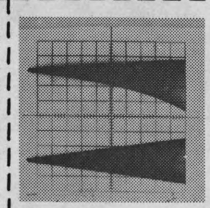	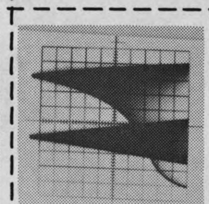	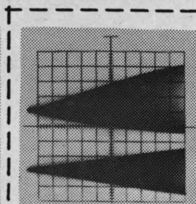

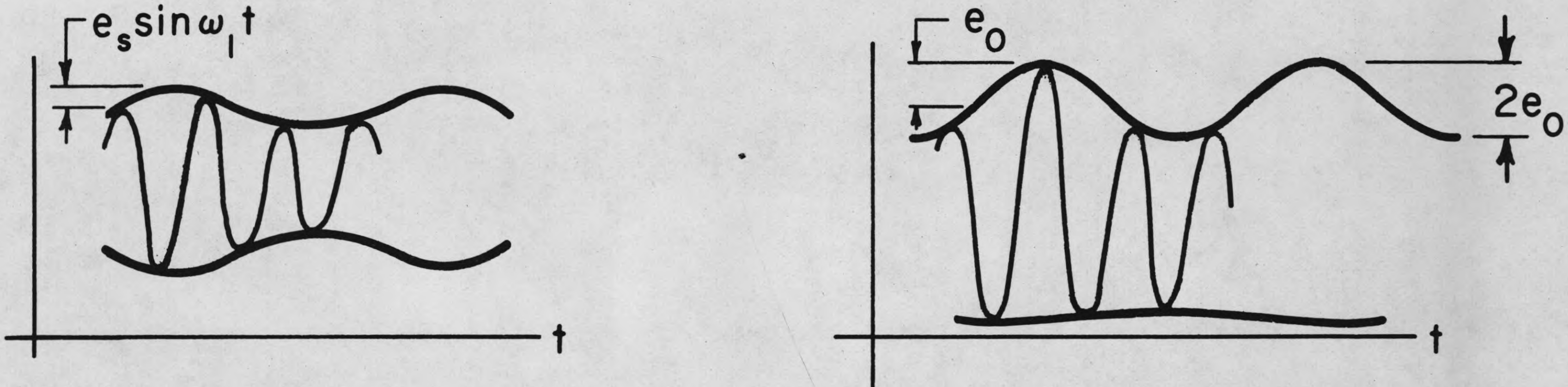

(a) $v_{s_{out}}$ (b) v_{out}

Fig. 16. Definition of e_s and e_o.

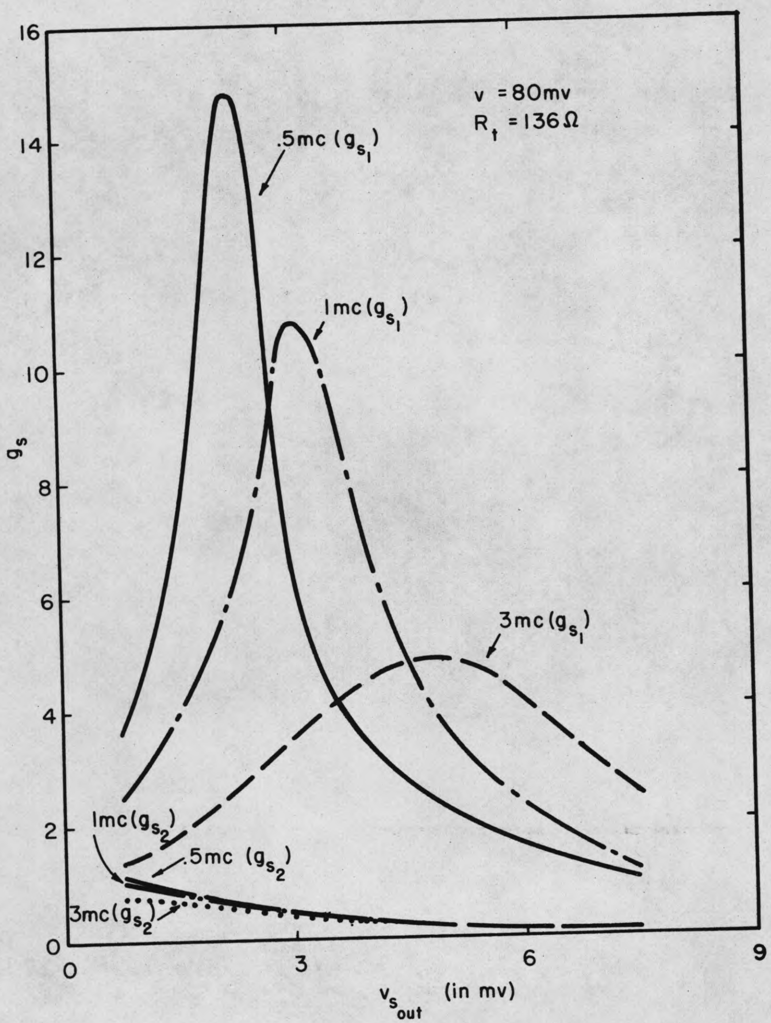

Fig. 17a. Small signal gain.

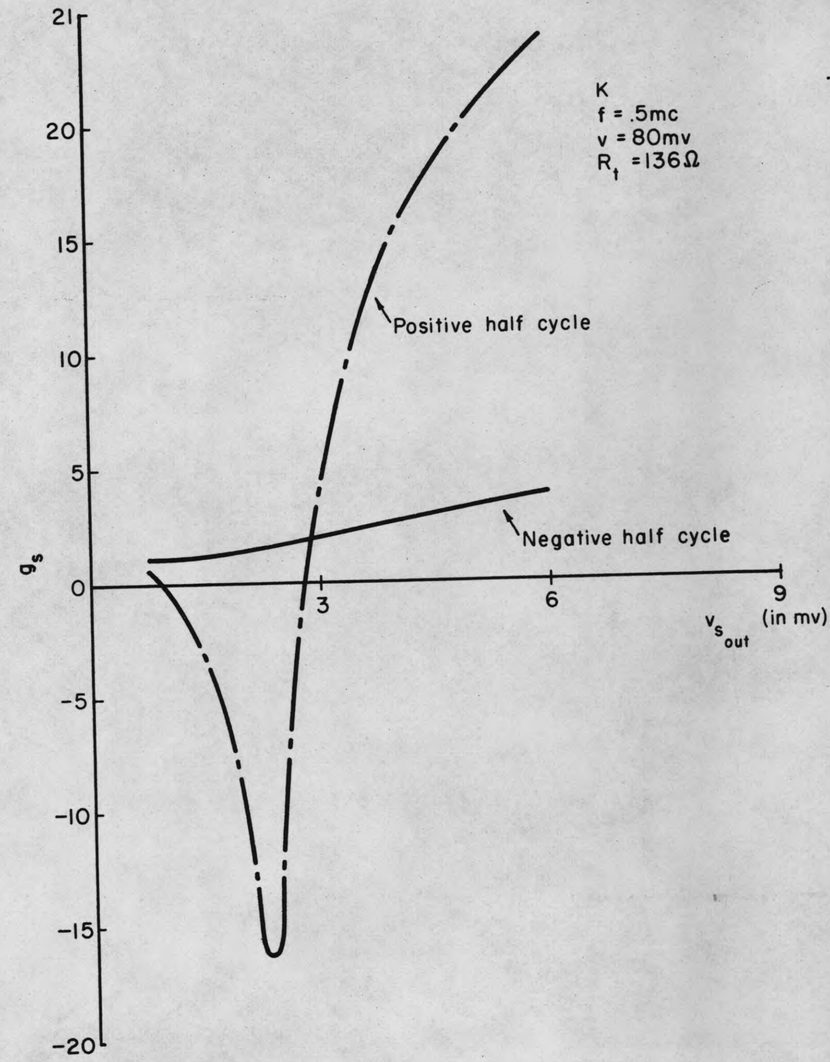

Fig. 17b. Gains of positive and negative half cycles.

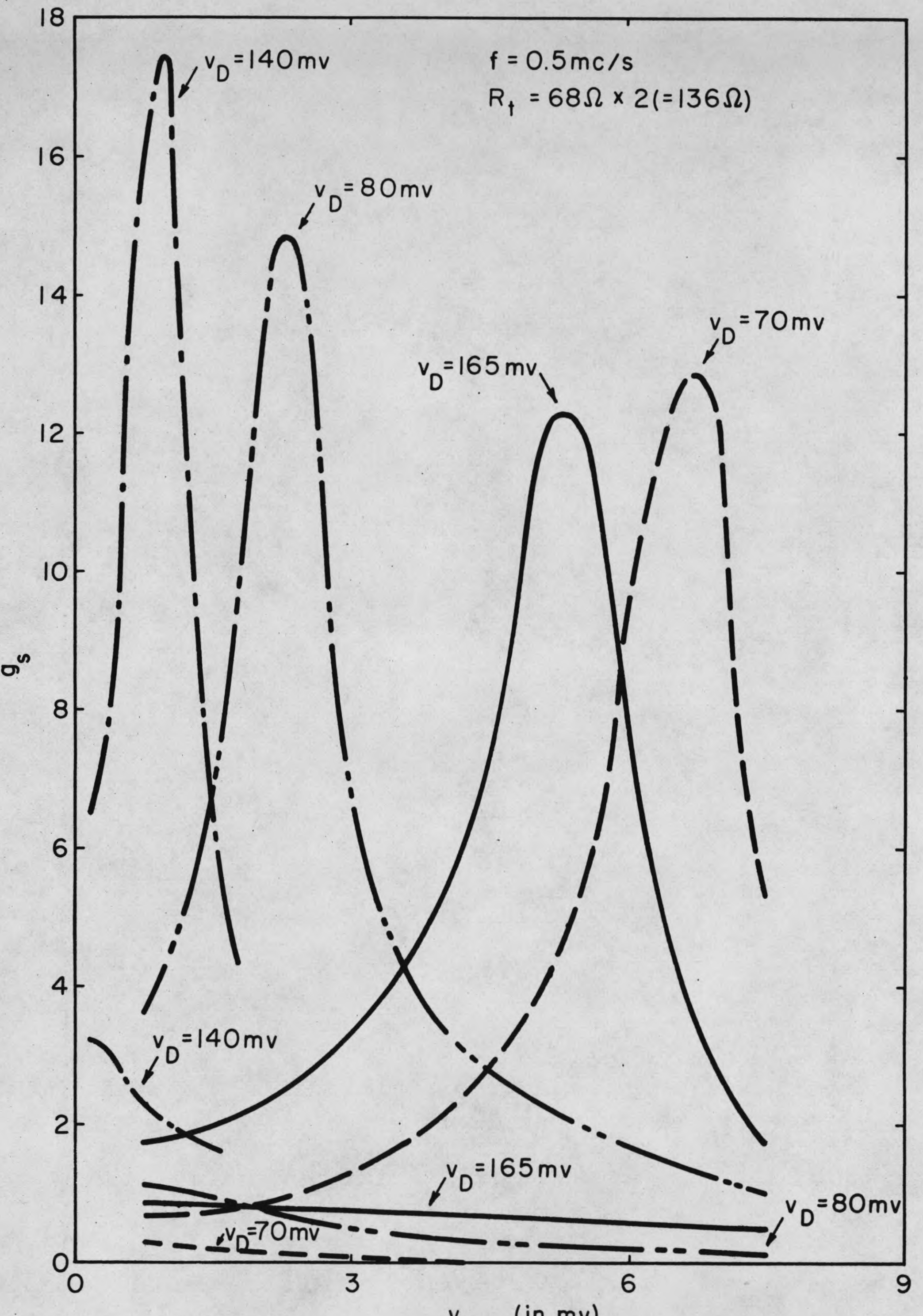

Fig. 18. Small signal gains with different V_D(voltage across the diode)

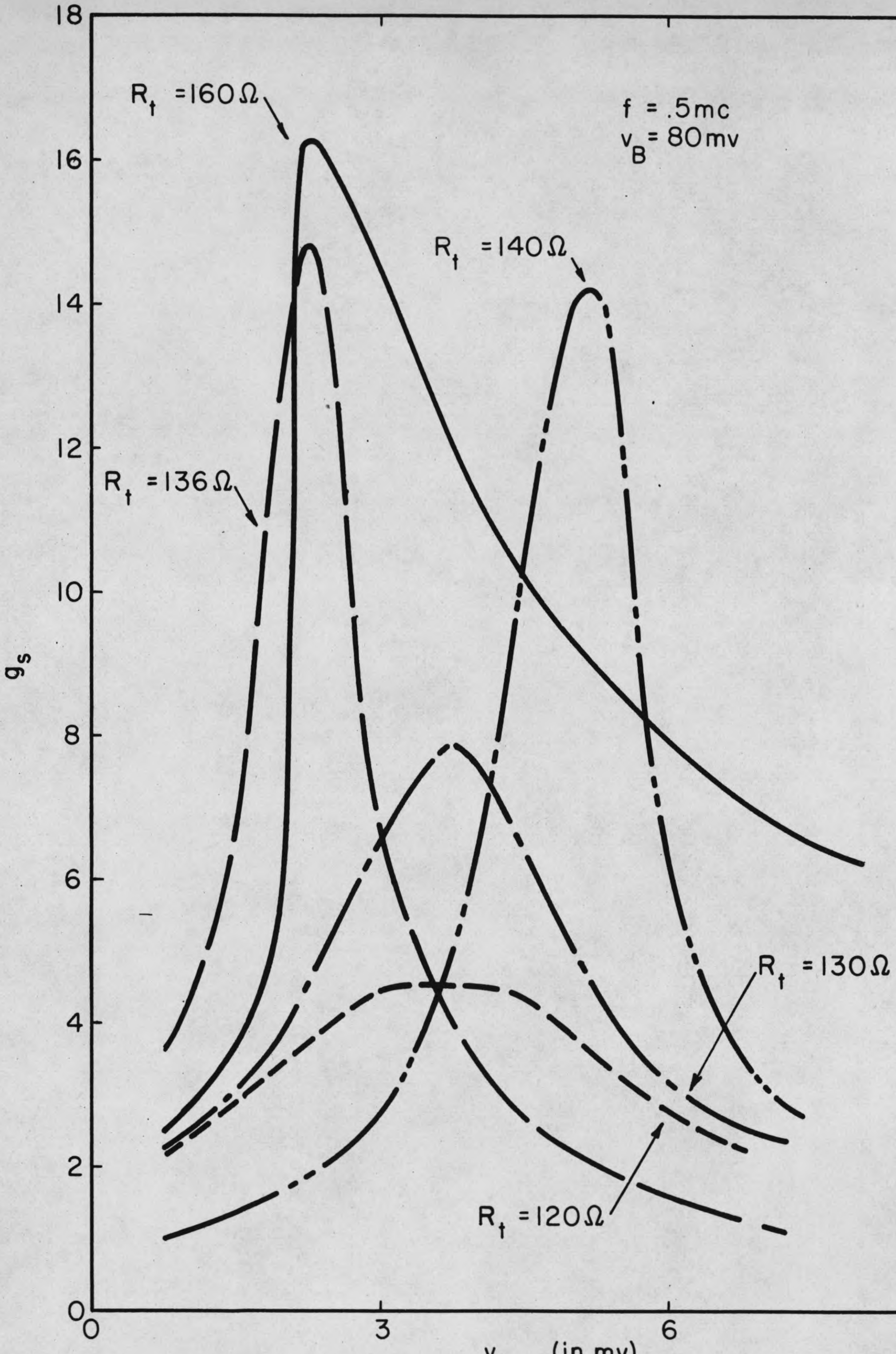

Fig. 19. Small signal gains with different R_t .

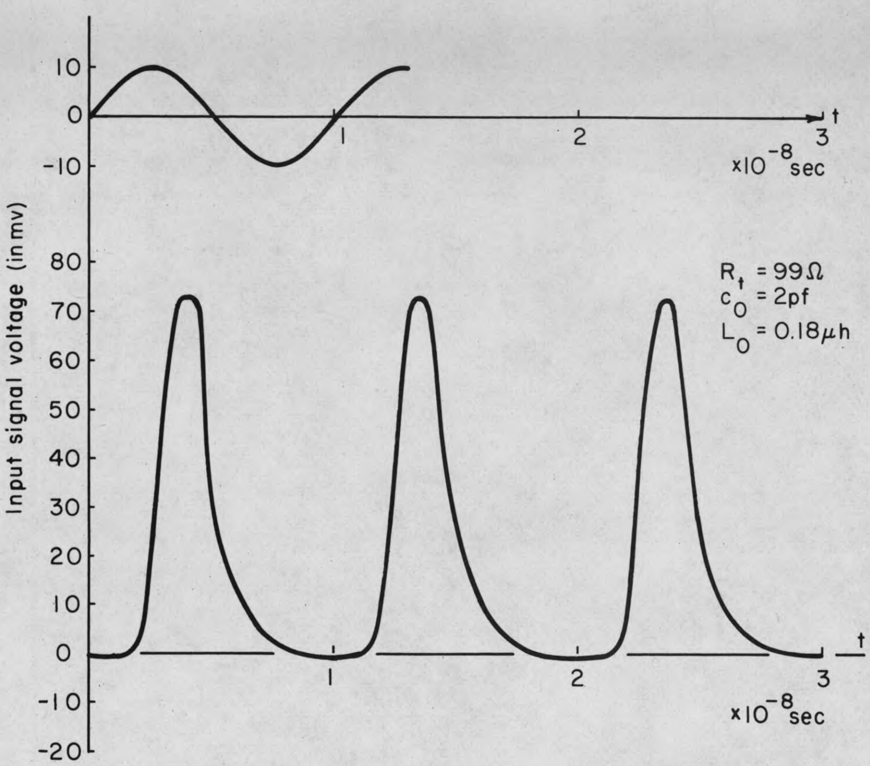

Fig. 21a. Waveform obtained by calculation.

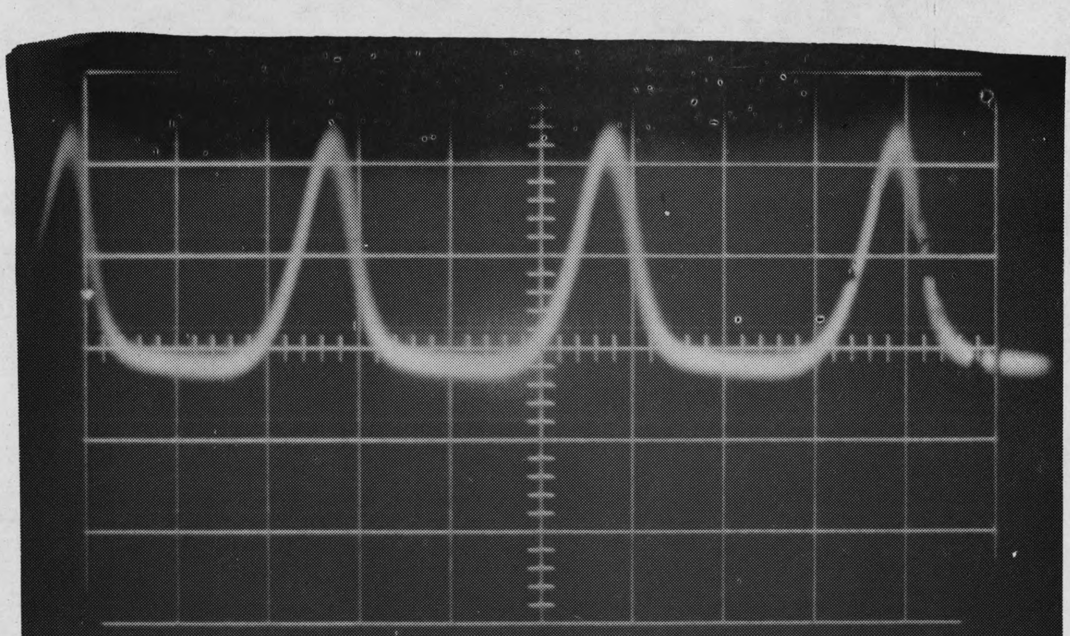

Fig. 21b. Waveform obtained by experiment.

REFERENCES

1. Chirlian, P. M., "A Technique for Cascading Tunnel Diode Amplifiers." Proc. of IRE, p. 1155, June 1960.

2. Hamann, D. R., "A Matched Amplifier Using Two Cascaded Esaki Diodes." Proc. of IRE, pp. 904-907, May 1961.

3. Long, E. D., and Womack, C. P., "Designing Tunnel Diode R-F Amplifiers." Electronics, pp. 120-123, February 1961.

4. Sard, E. W., "Tunnel (Esaki) Diode Amplifiers with Unusually Large Bandwidths." Proc. of IRE, pp. 357-358, March 1960.

5. Sie, J. J., "Absolutely Stable Hybrid, Coupled Tunnel-Diode Amplifier." Proc. of IRE, p. 1321, July 1960.

6. Trambarulo, R. F., "Esaki Diode Amplifiers at 7, 11, and 26 KMC." Proc. of IRE, pp. 2022-2023, December 1960.

7. Yariv, A., "Operation of an Easki Diode Microwave Amplifier." Proc. of IRE, p. 1155, June 1960.

8. Yariv, A., and Cook, J. S., "A Noise Investigation of Tunnel-Diode Microwave Amplifiers." Proc. of IRE, pp. 739-745, April 1961.

9. Dermit, G., Lockwood, H, and Hauer, W., "10.8-KMC Germanium Tunnel Diode." Proc. of IRE, pp. 519-520, February 1961.

10. Ko, Wen-Hsiung, "Designing Tunnel Diode Oscillators." Electronics, pp. 68-72, February 1961.

11. Sterzer, F., and Nelson, D. E., "Tunnel-Diode Microwave Oscillators." Proc. of IRE, pp. 744-753, April 1961.

12. Trambarulo, R., and Burrus, C. A., "Esaki Diode Oscillators from 3 to 40 KMC." Proc. of IRE, pp. 1776-1777, October 1960.

13. Bergman, R. H., "Tunnel Diode Logic Circuits." PGEC, pp. 430-438, December 1960.

14. Chow, W. F., "Tunnel Diode Logic Circuits." Electronics, pp. 101-107, June 1960.

15. Goto, E., "Esaki Diode High-Speed Logical Circuits." PGEC, pp. 25-29, March 1960.

16. Sims, R. C., Beck, E. R., Jr., and Kamm, V. C., "A Survey of Tunnel-Diode Digital Techniques." Proc. of IRE, pp. 136-145, January 1961.